Evidence for an Excitonic Insulator Phase in $1T$-$TiSe_2$

H. Cercellier,* C. Monney, F. Clerc, C. Battaglia, L. Despont, M. G. Garnier, H. Beck, and P. Aebi
Institut de Physique, Université de Neuchâtel, CH-2000 Neuchâtel, Switzerland

L. Patthey
Swiss Light Source, Paul Scherrer Institute, CH-5232 Villigen, Switzerland

H. Berger and L. Forró
Institut de Physique de la Matière Complexe, EPFL, CH-1015 Lausanne, Switzerland
(Received 30 March 2007; published 4 October 2007)

We present a new high-resolution angle-resolved photoemission study of $1T$-$TiSe_2$ in both its room-temperature, normal phase and its low-temperature, charge-density wave phase. At low temperature the photoemission spectra are strongly modified, with large band renormalizations at high-symmetry points of the Brillouin zone and a very large transfer of spectral weight to backfolded bands. A calculation of the theoretical spectral function for an excitonic insulator phase reproduces the experimental features with very good agreement. This gives strong evidence in favor of the excitonic insulator scenario as a driving force for the charge-density wave transition in $1T$-$TiSe_2$.

DOI: 10.1103/PhysRevLett.99.146403 PACS numbers: 71.10.−w, 71.35.Lk

Transition-metal dichalcogenides (TMDC's) are layered compounds exhibiting a variety of interesting physical properties, mainly due to their reduced dimensionality [1]. One of the most frequent characteristics is a ground state exhibiting a charge-density wave (CDW), with its origin arising from a particular topology of the Fermi surface and/or a strong electron-phonon coupling [2]. Among the TMDC's $1T$-$TiSe_2$ shows a commensurate $2 \times 2 \times 2$ structural distortion below 202 K, accompanied by the softening of a zone boundary phonon and with changes in the transport properties [3,4]. In spite of many experimental and theoretical studies, the driving force for the transition remains controversial. Several angle-resolved photoelectron spectroscopy (ARPES) studies suggested either the onset of an excitonic insulator phase [5,6] or a band Jahn-Teller effect [7]. Furthermore, $TiSe_2$ has recently attracted strong interest due to the observation of superconductivity when intercalated with Cu [8]. In systems showing exotic properties, such as Kondo systems, for example [9], the calculation of the spectral function has often been a necessary and decisive step for the interpretation of the ARPES data and the determination of the ground state of the systems. In the case of $1T$-$TiSe_2$, such a calculation for an excitonic insulator phase lacked so far.

In this Letter we present a high-resolution ARPES study of $1T$-$TiSe_2$, together with calculations of the excitonic insulator phase theoretical spectral function for this compound. We find that the experimental ARPES spectra show strong band renormalizations with a very large transfer of spectral weight into backfolded bands in the low-temperature phase. The spectral function calculated for the excitonic insulator phase is in strikingly good agreement with the experiments, giving strong evidence for the excitonic origin of the transition.

The excitonic insulator model was first introduced in the 1960s, for a semiconductor or a semimetal with a very small indirect gap E_G [10–13]. Thermal excitations lead to the formation of holes in the valence band and electrons in the conduction band. For low free carrier densities, the weak screening of the electron-hole Coulomb interaction leads to the formation of stable electron-hole bound states, called excitons. If the exciton binding energy E_B is larger than the gap energy E_G, the system becomes unstable upon formation of excitons. This instability can drive a transition to a coherent ground state of condensed excitons, with a periodicity given by the spanning vector $\mathbf{w}$ that connects the valence band maximum to the conduction band minimum. In the particular case of $TiSe_2$, there are three vectors $(\mathbf{w}_i, i = 1, 2, 3)$ connecting the Se $4p$-derived valence band maximum at the Γ point to the three symmetry-equivalent Ti $3d$-derived conduction band minima at the L points of the Brillouin zone (BZ) [see inset of Fig. 1(b)].

Our calculations are based on the BCS-like model of Jérome, Rice, and Kohn [12], adapted for multiple $\mathbf{w}_i$. The band dispersions for the normal phase have been chosen of the form

$$\begin{aligned} \epsilon_v(\mathbf{k}) &= \epsilon_v^0 + \hbar^2 \frac{k_x^2 + k_y^2}{2m_v} + t_v \cos\left(\frac{2\pi k_z}{c}\right) \\ \epsilon_c^i(\mathbf{k}, \mathbf{w}_i) &= \epsilon_c^0 + \hbar^2 \left(\frac{(k_x - w_{ix})^2}{2m_c^x} + \frac{(k_y - w_{iy})^2}{2m_c^y}\right) \\ &\quad + t_c \cos\left(\frac{2\pi(k_z - w_{iz})}{c}\right) \end{aligned} \tag{1}$$

for the valence (ϵ_v) and the three conduction (ϵ_c^i) bands, respectively, with c the lattice parameter perpendicular to the surface in the normal $(1 \times 1 \times 1)$ phase, t_v and t_c the amplitudes of the respective dispersions perpendicular to the surface, and m_v, m_c the effective masses.

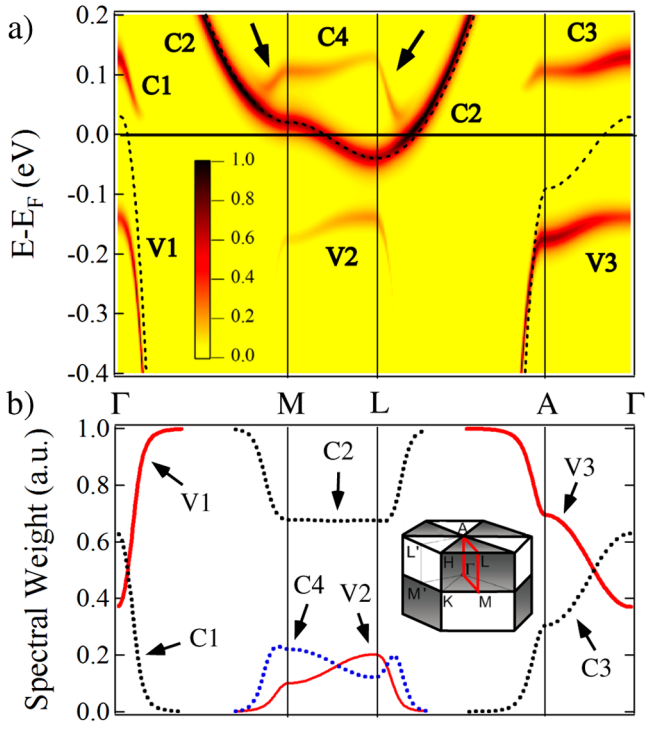

FIG. 1 (color online). (a) Theoretical spectral function of the excitonic insulator in a $1T$ structure, calculated for the band structure described in the text and an order parameter $\Delta = 0.075$ eV. The $V1$–$V3$ (respectively, $C1$–$C4$) branches refer to the valence (respectively, conduction) band. Dashed lines correspond to the normal phase ($\Delta = 0$). The path in reciprocal space is shown in red (or gray) in the inset. (b) Spectral weight of the different bands. Inset: bulk Brillouin zone of $1T$-$TiSe_2$.

Within this model one-electron Green's functions were calculated for the excitonic insulator phase. For the valence band, one obtains

$$G_v(\mathbf{k}, z) = \left(z - \epsilon_v(\mathbf{k}) - \sum_{\mathbf{w}_i} \frac{|\Delta|^2(\mathbf{k}, \mathbf{w}_i)}{z - \epsilon_c(\mathbf{k} + \mathbf{w}_i)}\right)^{-1}. \quad (2)$$

This is a generalized form of the equations of Ref. [12] for an arbitrary number of $\mathbf{w}_i$. The order parameter Δ is related to the number of excitons in the condensed state at a given temperature. For the conduction band, the Green's functions G_c^i corresponding to each spanning vector $\mathbf{w}_i$ is

$$G_c^i(\mathbf{k} + \mathbf{w}_i, z) = \left(z - \epsilon_c(\mathbf{k} + \mathbf{w}_i) - \frac{|\Delta|^2(\mathbf{k}, \mathbf{w}_i)}{z - \epsilon_v(\mathbf{k}) - \sum_{j \neq i} \frac{|\Delta|^2(\mathbf{k}, \mathbf{w}_j)}{z - \epsilon_c(\mathbf{k} + \mathbf{w}_j)}}\right)^{-1} \quad (3)$$

This model and the derivation of the Green's functions will be further described in a forthcoming paper [14].

The parameters for Eqs. (1) were derived from photon energy dependent ARPES measurements carried out at the Swiss Light Source on the SIS beam line, using a Scienta SES-2002 spectrometer with an overall energy resolution better than 10 meV, and an angular resolution better than 0.5°. The fit to the data gives for the Se $4p$ valence band a maximum $+30 \pm 10$ meV, and for the Ti $3d$ conduction band a minimum -40 ± 5 meV with respect to the Fermi energy E_F [15], yielding a semimetallic band structure with a negative gap (i.e., an overlap) $E_G = -70 \pm 15$ meV for the normal phase of $TiSe_2$, in agreement with the literature [16].

The spectral function calculated along several high-symmetry directions of the BZ is shown in Fig. 1(a), for a zero order parameter (dashed lines) and for an order parameter $\Delta = 0.075$ eV. This value has been chosen for best agreement with experiment. The color scale shows the spectral weight carried by each band. For presentation purposes the δ-like peaks of the spectral function have been broadened by adding a constant 30 meV imaginary part to the self-energy. In the normal phase (dashed lines), as previously described we consider a semimetal with a 70 meV overlap, with bands carrying unity spectral weight. In the excitonic phase, the band structure is strongly modified. The first observation is the appearance of new bands (labeled $C1$, $V2$, $C3$, and $C4$), backfolded with the spanning vector $\mathbf{w} = \Gamma L$. The $C1$, $C3$, and $V2$ branches are the backfolded replicas of branches $C4$ and $V3$, respectively. In this new phase the Γ and L points are now equivalent (in the sense that the poles of the Green's functions are the same, but not the spectral weight), which means that the excitonic state has a $2 \times 2 \times 2$ periodicity of purely electronic origin, as expected from theoretical considerations [10,12]. Another effect of exciton condensation is the partial opening of a gap in the excitation spectrum. This results in a flattening of the valence band near Γ in the ΓM direction ($V1$ branch) and in the $A\Gamma$ direction ($V3$ branch), and also an upward bend of the conduction band near L and M ($C4$ branch). It is interesting to notice that the splitting of the conduction band in two contributions ($C2$ and $C4$) near M and L results from the backfolding of the L points onto each other, according to the new periodicity of the excitonic state (see Fig. 8 in Ref. [17]). The spectral weight carried by the bands is shown in Fig. 1(b). The largest variations occur near the Γ, A, L, and M points, where the band extrema in the normal phase are close enough for excitons to be created. Away from these points, the spectral weight decreases in the backfolded bands ($C1$, $V2$, $C3$, and $C4$) and increases in the others. The intensity of the $V1$ branch, for example, decreases by 60% when approaching Γ, whereas the backfolded $C1$ branch shows the opposite behavior. Such a large transfer of spectral weight into the backfolded bands is a very uncommon and striking feature. Indeed, in most compounds with competing potentials (CDW systems, vicinal surfaces, and so on), the backfolded bands carry an extremely small spectral weight [18–20]. In these systems the backfolding results mainly from the influence of the modified lattice on the electron gas, and the weight transfer is related to the strength of the new crystal potential component. Here, the case of the excitonic insulator is completely different, as the backfolding is an intrinsic property of the excitonic state. The

large transfer of spectral weight is then a purely electronic effect, and turns out to be a characteristic feature of the excitonic insulator phase.

Figure 2 shows ARPES spectra recorded at a photon energy $h\nu = 31$ eV as a function of temperature. At this photon energy, the normal emission spectra correspond to states located close to the Γ point. For the sake of simplicity the description is in terms of the surface BZ high-symmetry points $\bar{\Gamma}$ and $\bar{M}$. The 250 K spectra exhibit the three Se $4p$-derived bands at $\bar{\Gamma}$ and the Ti $3d$-derived band at $\bar{M}$ widely described in the literature [5–7]. The thick dotted lines (white) are fits by Eq. (1), giving for the topmost $4p$ band an apparent maximum energy of -20 ± 10 meV, and for the Ti $3d$ a minimum energy of -40 ± 5 meV at this temperature. We speak here of an apparent maximum energy for the valence band, as the system appears already affected by excitonic fluctuations. Indeed, on the 250 K spectrum at $\bar{\Gamma}$, the intensity is low near normal emission. This reduced intensity and the residual intensity at $\bar{M}$ around 150 meV binding energy (arrows) may arise from exciton fluctuations [see reduction of spectral weight near Γ in the $V1$ branch in Fig. 1(b)]. Matrix elements appear to play a minor role as the intensity variation depends only very slightly on photon energy and polarization, and is also observed in the second Brillouin zone. In the 65 K data [Fig. 2(b)], the topmost $4p$ band flattens near $\bar{\Gamma}$ and shifts to higher binding energy by about 100 meV (thin white, dotted line). This shift is accompanied by a larger decrease of the spectral weight near the top of the band. The two other bands (fine black lines) are only slightly shifted. Intuitively this can be understood by the fact that these bands are farther away from E_F and therefore less involved by the interaction. In the $\bar{M}$ spectrum strong backfolded valence bands can be seen, and the conduction band shows significant intensity variations, with a maximum intensity located about 0.25 Å^{-1} from $\bar{M}$. This observation is in agreement with Kidd *et al.* [6], although in their case the conduction band was unoccupied in the normal phase. This difference is due to a slight Ti overdoping of our samples [3]. In our case, the 2×2 CDW was found to appear at 180 ± 10 K from scanning tunneling microscopy measurements, indicating a Ti doping of less than 1%. However, a 40 meV binding energy for the conduction band is still consistent with the excitonic insulator scenario, as the exciton binding energy is expected to be close to that value [5,6].

Spectral functions calculated for the same $k_{\|}$ as the data of Fig. 2 are shown in Fig. 3. Only the Γ and L points are shown, as the excitonic effects are more important near these points. For comparison with Fig. 2 we refer to the projection of these points on the surface BZ $\bar{\Gamma}$ and $\bar{M}$. The effect of temperature was taken into account via the order parameter and the Fermi function. In order to understand

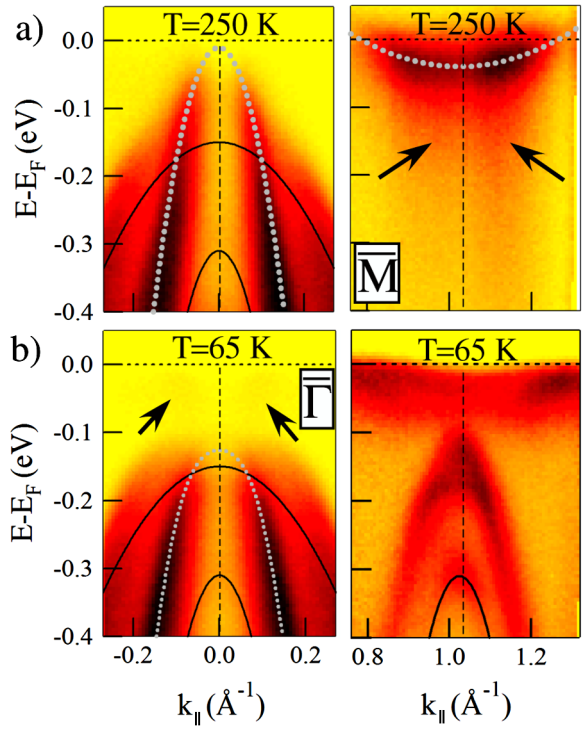

FIG. 2 (color online). ARPES spectra of $1T$-$TiSe_2$ for (a) above and (b) below the CDW transition temperature. Thick dotted lines are parabolic fits to the bands in the normal phase and thin dotted lines are guides to the eye for the CDW phase. Fine lines follow the dispersion of the $4p$ sidebands (see text).

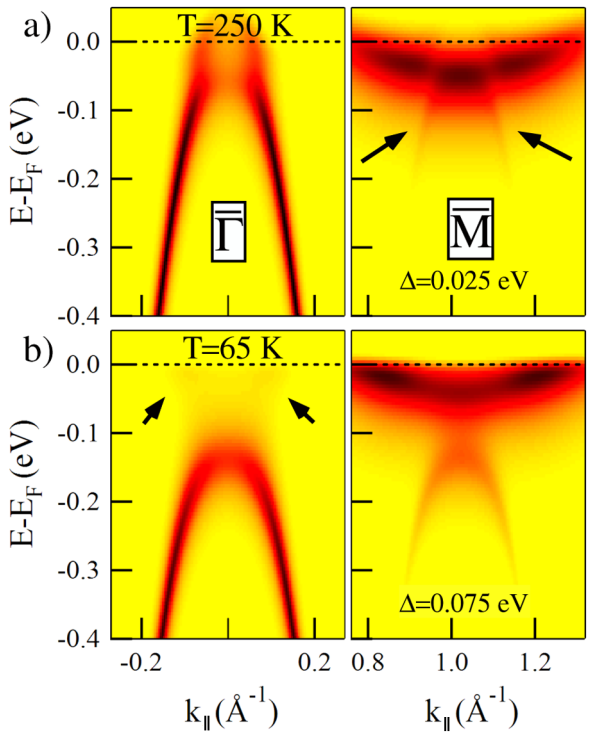

FIG. 3 (color online). Theoretical spectral function of $1T$-$TiSe_2$ in the vicinity of Γ and L. (a) above and (b) below the CDW transition temperature (see text). For comparison with Fig. 2 we refer to the projection of these points on the surface BZ $\bar{\Gamma}$ and $\bar{M}$.

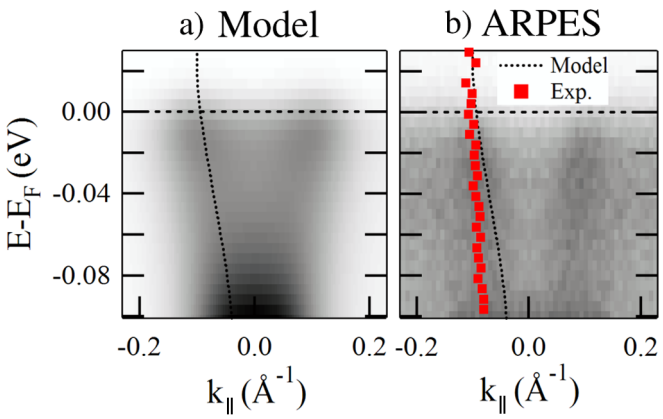

FIG. 4 (color online). Near-E_F spectral function in the vicinity of the Γ point. The theoretical data correspond to Fig. 3(b) and the ARPES to Fig. 2(b) (see arrows on these figures).

the detailed behavior of the ARPES spectra, a three band model would be necessary. However, considering only the topmost valence band allows us to reproduce the essential features of the ARPES data. Indeed, the behavior of this band is extremely well reproduced by the calculation. In the 250 K calculation an effective order parameter of 25 meV was used to account for the fluctuation effects. This allows us to reproduce the intensity loss near $\bar{\Gamma}$ and the appearance of spectral weight at $\bar{M}$ (arrows). In the 65 K calculation the valence band is flattened near $\bar{\Gamma}$, and the spectral weight at this point is reduced to 39%, close to the experimental value of 35%. The agreement is very satisfying, considering that the calculation takes into account only the lowest excitonic state.

In the near-$\bar{M}$ spectral function, the backfolded valence band is strongly present in the 65 K calculation. The conduction band maximum intensity is located away from $\bar{M}$ as in the experiment. It is important to notice that the ARPES spectra show no significant shift of the conduction band related to atomic displacements in the distorted phase [6,7,21]. Such atomic displacements, in terms of a band Jahn-Teller effect, were suggested as a driving force for the transition. However, the key point is that, although the lattice distortion may shift the conduction band, the very small atomic displacements ($\approx$0.02 Å [3]) in 1T-$TiSe_2$ are expected to lead to a negligible spectral weight in the backfolded bands [20]. As an example, 1T-TaS_2, another CDW compound known for very large atomic displacements [22] (of order $>$0.1 Å) introduces hardly detectable backfolding of spectral weight in ARPES. Clearly, an electronic origin is necessary for obtaining such strong backfolding in the presence of such small atomic displacements. Therefore, our results allow us to rule out a Jahn-Teller effect as the driving force for the transition of $TiSe_2$.

Furthermore, the ARPES spectra also show evidence for the backfolded conduction band at the $\bar{\Gamma}$ point. Figure 4 shows spectra around the Fermi energy, taken from the data of Figs. 2(b) and 3(b) (arrows). In the ARPES data two slightly dispersive peaks clearly cross the Fermi level. The experimental dispersion of these peaks [red (or gray) squares] is well reproduced in the calculation (dotted lines). These features turn out to be the populated tail of the backfolded conduction band, whose centroid is located just above the Fermi level. To our knowledge no evidence for the backfolding of the conduction band had been put forward so far.

In summary, by comparing ARPES spectra of 1T-$TiSe_2$ to theoretical predictions for an excitonic insulator, we have shown that the $2 \times 2 \times 2$ periodicity induced by the exciton condensate results in a very large transfer of spectral weight into backfolded bands. This effect, clearly evidenced by photoemission, turns out to be a characteristic feature of the excitonic insulator phase, thus giving strong evidence for the existence of this phase in 1T-$TiSe_2$ and its prominent role in the CDW transition.

Skillfull technical assistance was provided by the workshop and electric engineering team. This work was supported by the Fonds National Suisse pour la Recherche Scientifique through Div. II and MaNEP.

*herve.cercellier@grenoble.cnrs.fr

[1] J. A. Wilson *et al.*, Adv. Phys. **24**, 117 (1975).
[2] F. Clerc *et al.*, Phys. Rev. B **74**, 155114 (2006).
[3] F. J. Di Salvo *et al.*, Phys. Rev. B **14**, 4321 (1976).
[4] M. Holt *et al.*, Phys. Rev. Lett. **86**, 3799 (2001).
[5] T. Pillo *et al.*, Phys. Rev. B **61**, 16 213 (2000).
[6] T. E. Kidd *et al.*, Phys. Rev. Lett. **88**, 226402 (2002).
[7] K. Rossnagel *et al.*, Phys. Rev. B **65**, 235101 (2002).
[8] E. Morosan *et al.*, Nature Phys. **2**, 544 (2006).
[9] D. Malterre *et al.*, Adv. Phys. **45**, 299 (1996).
[10] W. Kohn, Phys. Rev. Lett. **19**, 439 (1967).
[11] B. I. Halperin and T. M. Rice, Rev. Mod. Phys. **40**, 755 (1968).
[12] D. Jérome *et al.*, Phys. Rev. **158**, 462 (1967).
[13] F. X. Bronold and H. Fehske, Phys. Rev. B **74**, 165107 (2006).
[14] C. Monney *et al.* (to be published).
[15] The fit parameters are $\epsilon_v^0 = -0.03 \pm 0.005$ eV, $m_v = -0.23 \pm 0.02 m_e$, where m_e is the free electron mass, $t_v = 0.06 \pm 0.005$ eV; $\epsilon_c^0 = -0.01 \pm 0.0025$ eV, $m_c^x = 5.5 \pm 0.2 m_e$, $m_c^y = 2.2 \pm 0.1 m_e$, $t_c = 0.03 \pm 0.0025$ eV.
[16] O. Anderson *et al.*, Phys. Rev. Lett. **55**, 2188 (1985).
[17] J. A. Wilson *et al.*, Phys. Rev. B **18**, 2866 (1978).
[18] C. Didiot *et al.*, Phys. Rev. B **74**, 081404(R) (2006).
[19] C. Battaglia *et al.*, Phys. Rev. B **72**, 195114 (2005).
[20] J. Voit *et al.*, Science **290**, 501 (2000).
[21] M. H. Whangbo and E. Canadell, J. Am. Chem. Soc. **114**, 9587 (1992).
[22] A. Spijkerman *et al.*, Phys. Rev. B **56**, 13 757 (1997).